Paper 252

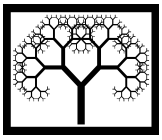

Proceedings of the Eleventh International Conference
on Computational Structures Technology,
B.H.V. Topping, (Editor),
Civil-Comp Press, Stirlingshire, Scotland

Representation of Localized Phenomena in Dynamics using Multi-Scale Coupling

J. Marchais, C. Rey and L. Chamoin
LMT-Cachan
(ENS Cachan/CNRS/UPMC/PRES UniverSud Paris)
Cachan, France

Abstract

In this paper we introduce a multiscale method in dynamics using both a nonlocal discrete model and an local continuum model. The issue in such a method is the numerical reflections arising from the nonlocal/local and the fine/coarse interfaces. Therefore, our method introduces accurate reconstruction schemes based on the quasi-continuum method, as well as absorbing conditions based on a scale decomposition combined to a perfectly matched layer, to eliminate these suprious phenomena.

Keywords: multi-scale modelling, nonlocal discrete model, scale decomposition, quasi-continuum method, ghost forces, dynamics, damping.

1 Introduction

Nonlocal discrete models are a prominent tool in Computational Mechanics for describing fiber reinforced concrete as well as composite or nanometerials. Indeed, they enable to reveal complex physical phenomena such as solid fracture, plasticity or damage [1]. The nonlocal aspect is due to the interaction range defined on each particle. Hence, particles interact by means of potentials like Lennard-Jones, Morse, etc, with each particle included in its interaction range. However, due to the space and time degrees of freedom necessary, such models are limited to localized regions in which the particle scale is important. In the remainder of the domain, a reduction method based on continuum simulations is used, which allows simulations at larger space and time scales. Consequently, multiscale methods coupling nonlocal discrete model and continuum mechanics are required (see [2]) and the difficulty lies on the intimate and accurate coupling so that the critical region behaves as if the entire model were nonlocal and discrete.

In order to couple a discrete nonlocal model with a continuum local model in dy-

namics, we can define two steps: (i) the first one is to couple a nonlocal discrete model with a local discrete model (ii) the second one is to couple a local discrete model with continuum a local model. Hence, two approaches can be distinguished to couple different models:

- surface coupling using a discrete interface: Mortar method, edge-to-edge coupling, Quasi-Continuum method [3][4]...
- volume coupling using an overlaping zone: Bridging Domain method [5][6], Chimera method, Bridging Scale method [7],...

The work presented here deals with both steps, step (i) by means of the Quasi-continuum method and step (ii) by means of a scale decomposition.

The QC method used for step (i) generates local/nonlocal interface where the local discrete model is homogenized from the nonlocal model by using the Cauchy-Born rule. Nevertheless, undesired forces called "ghost forces" [8, 9] appear in this method, which are responsible, in dynamics, for spurious reflections at the interfaces that pollute the whole simulation. We provide consistent schemes [10] for the QC methods where the local/nonlocal interfaces between models remain free from "ghost forces". Step (ii) leads to couple macro and micro scales. In dynamics, a part of the micro scale is not represented by the macro scale which also generates spurious reflexions at the interfaces. Hence, we develop a new discrete/continnum interface, based on a scale decomposition coupled to Perfectly Matched Layer [11, 13] permeable for macro waves and absorbing for micro waves.

2 Local/nonlocal interfaces

In this section, we introduce the discrete nonlocal model. We then show how to obtain a local equivalent discrete model and how to deal with local/nonlocal interfaces using geometrically consistent QC-type approximation. Finally, we run some dynamics simulations on 2D problems to highlight the gain on the reduction of spurious reflections.

2.1 The discrete nonlocal model

The discrete aspect is due to the fact that the material is represented through a lattice of N discrete particles. In the reference configuration, the position $\mathbf{X}_i$ of each particle i is written :

$$\mathbf{X}_i = \sum_{l=1}^{d} A_i^l \mathbf{e}_l \quad \text{with} \quad \left(A_i^1, ..., A_i^d\right) \in \mathbb{Z}^d, \tag{1}$$

where $\{\mathbf{e}_l\}_{l=1,...,d}$ are known as the d primitive vectors of a d-dimensional (d=1,2 or 3) problem. Let $\mathbf{x}_i$ be the position of the particle i in the current deformed configura-

tion. Then, the behavior of the material relies on the interactions E_{ij} defined between particles, with E_{ij} a pairwise potential such that

$$E_{ji} = E_{ij} = E_{ij}\left(\mathbf{r}_i^a(j)\right) \quad \text{with} \quad \mathbf{r}_i^a(j) = \mathbf{x}_j - \mathbf{x}_i, \tag{2}$$

Harmonic, Lennard-Jones or Morse potentials are some examples of pairwise potentials that can be used to describe the material behavior. Hence, the nonlocal aspect of the model is due to the interaction range r_c between particles which includes particles beyond first neighbors (see Figure 1). Finally, the total energy E^{tot} of the model is given by

$$E^{tot} = \sum_{i=1}^{N} E_i^a\left(\{\mathbf{x}_i\}\right) \quad \text{with} \quad E_i^a = \frac{1}{2}\sum_{j\neq i} E_{ij}\left(\mathbf{r}_i^a(j)\right), \tag{3}$$

where E_i^a denotes the nonlocal energy associated to the i-th particle [4].

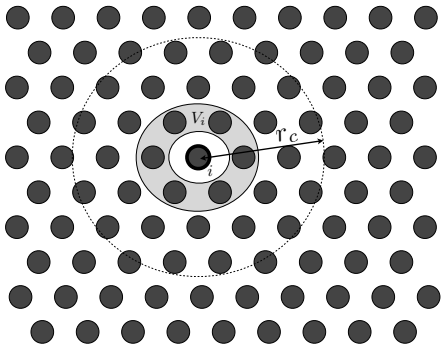

Figure 1: 2D discrete model

2.2 The local QC approximation

The aim of the local QC approximation is to define a local equivalent energy E_i^{CB} by replacing all next-nearest neighbor interactions by nearest neighbor (denoted V_i) interactions. In order to do so, a local reconstruction scheme $\mathbf{r}_i^{CB}(j)$ based on the Cauchy-Born rule is introduced :

$$\mathbf{R}_i(j) = \mathbf{X}_j - \mathbf{X}_i = \sum_{l\in V_i} \alpha_i^l(j)\left(\mathbf{X}_l - \mathbf{X}_i\right) \tag{4}$$

$$\Longrightarrow \mathbf{r}_i^a(j) \approx \mathbf{r}_i^{CB}(j) = \sum_{l\in V_i} \alpha_i^l(j)\left(\mathbf{x}_l - \mathbf{x}_i\right), \tag{5}$$

where coefficients $\left\{\alpha_i^l(j)\right\}_{l=1,\dots,d}$ only depend on the geometry of the lattice and are all positive. Note, that we use a protocol that only selects the *closest* particles of V_i to obtain a unique set of particles in V_i that can define the local reconstruction scheme

$\mathbf{r}_i^L(j)$. Hence, combining (3) and (5) we obtain the formulation of the local equivalent energy :

$$E_i^{CB} = \frac{1}{2}\sum_{j\neq i} E_{ij}\left(\mathbf{r}_i^{CB}(j)\right). \tag{6}$$

Under the assumption of a uniform deformation, the local QC approximation is consistent if this reconstruction is used on all particles [9]. Nevertheless, if we use both local and nonlocal definition of the energy to obtain a local and a nonlocal domain, some spurious phenomena so-called *ghost forces* arise along interfaces [3, 8, 9].

2.3 A geometrically consistent QC-type approximation : NL2L scheme

In order to be able to deal with local/nonlocal interfaces, we use a geometrically consistent QC-type approximation, called NL2L scheme, defined in [10]. The idea is to add a transition domain between local and nonlocal domains, respectively denoted $\mathcal{J}_l$ and $\mathcal{J}_a$. Hence, we use a row of quasi-nonlocal particles that define the interface denoted $\mathcal{J}_b$ that follows the QNL scheme of [8]:

$$E_i^{Q} = \frac{1}{2}\sum_{j\in\mathcal{J}_a} E_{ij}\left(\mathbf{r}_i^a(j)\right) + \frac{1}{2}\sum_{j\in\mathcal{J}_l\cup\mathcal{J}_b} E_{ij}\left(\mathbf{r}_i^{CB}(j)\right). \tag{7}$$

Then, we introduce the reconstruction scheme $\mathbf{r}_i^b(j)$ based on particles included in $\mathcal{J}_b$ such that

$$\mathbf{R}_i(j) = \mathbf{X}_j - \mathbf{X}_i = \sum_{l\in\mathcal{J}_b} \alpha_i^l(j)\left(\mathbf{X}_l - \mathbf{X}_i\right) \tag{8}$$

$$\Longrightarrow \mathbf{r}_i^a(j) \approx \mathbf{r}_i^b(j) = \sum_{l\in\mathcal{J}_b} \alpha_i^l(j)\left(\mathbf{x}_l - \mathbf{x}_i\right). \tag{9}$$

We denote by $\mathcal{J}_{b,nl}$ the particles close to the interface which have at least one interaction with a particle in $\mathcal{J}_l$. Hence, for these particles, we use the QC-type approximation defined in [10] :

$$E_i^{QC} = \frac{1}{2}\sum_{j\in\mathcal{J}_l} \frac{-2}{\sum_{l\in\mathcal{J}_b}\alpha_i^l(j)} E_{ij}\left(\mathbf{r}_i^b(j)\right) + \frac{1}{2}\sum_{j\in\mathcal{J}_l\cup\mathcal{J}_a} E_{ij}\left(\mathbf{r}_i^a(j)\right). \tag{10}$$

Note that the size of the intermediate domain $\mathcal{J}_{b,nl}$ corresponds to the size of the interaction range r_c. The total energy of the model (3) can be rewritten :

$$E^{tot} = \sum_{i\in\mathcal{J}_l} E_i^{CB} + \sum_{i\in\mathcal{J}_b} E_i^{Q} + \sum_{i\in\mathcal{J}_a} E_i^{a} + \sum_{i\in\mathcal{J}_{b,nl}} E_i^{QC}. \tag{11}$$

Finally, we obtain a geometrically consistent QC-type approximation that is free from *ghost forces* whatever the interaction range or the potential used. Moreover, under some precautions, it is possible to handle cases with corner [10] between the local and nonlocal domain.

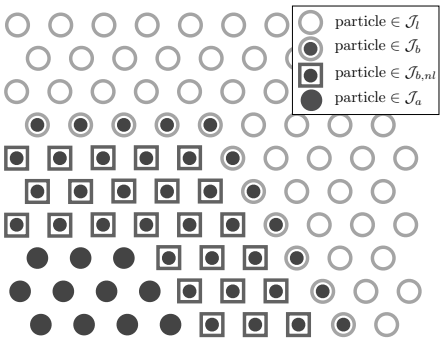

Figure 2: The four kinds of particles of the NL2L scheme

2.4 Applications on dynamics problems

The gain on the accuracy obtained with such a QC-type approximation has been shown in [10] for statics problems. Moreover it appears that it also reduces spurious reflexions in dynamics . Hence, we want to study the gain obtained on 2D problems with several local/nonlocal interfaces.

In order to do so, we use an hexagonal lattice that includes 121×121 particles. The interaction range on each particle includes particles up to the 8^{th} neighbor, which corresponds to $r_c = 4r_0$ with r_0 the distance between the first neighbors on the reference configuration. Then, the interactions between particles are represented through harmonic potentials such that

$$E_{ij}(\mathbf{r}_i(j)) = \frac{1}{2} k_{ij} \left(|\mathbf{r}_i(j)| - |\mathbf{R}_i(j)| \right)^2 . \tag{12}$$

Finally the nonlocal domain, including 29×29 particles, is confined in the center of the sample as defined in Figure 3.

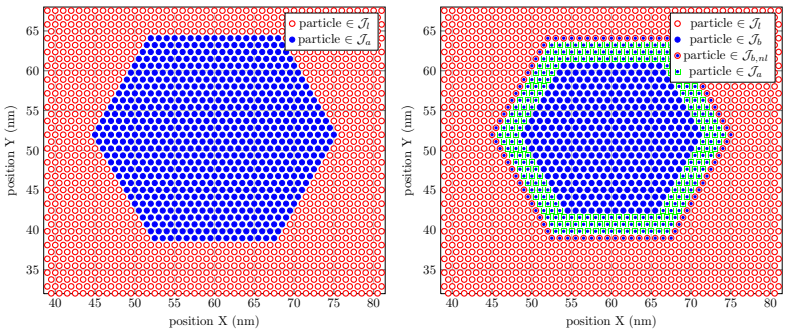

(a) QNL scheme (b) NL2L scheme

Figure 3: Zoom in the nonlocal domain

Figure 4 illustrates the initial displacement imposed along the x direction such that the initial energy is only included in the nonlocal domain. Then we run simulations

with both inconsistent and consistent QC-type approximations to see how the waves spreads over the local/nonlocal interfaces.

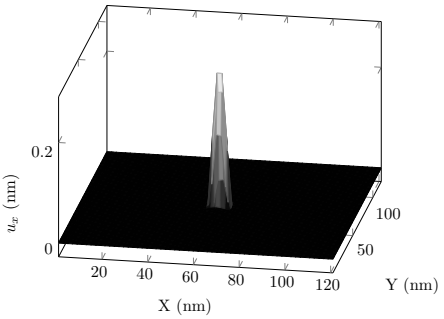

Figure 4: Initial u_x displacement

The energy repartition in time highlights the reflections due to local/nonlocal interfaces. Indeed, it appears in Figure 5 that more than 40% of the energy remains trapped in the nonlocal domain when using the QNL scheme at local/nonlocal interfaces. Such reflections are avoided with the NL2L scheme, indeed less than 10% of the energy remains in the nonlocal domain.

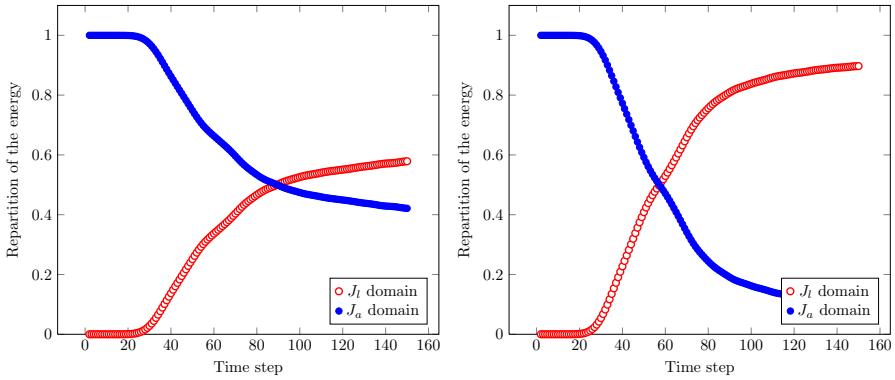

(a) Inconsistent QC-approximation (b) Consistent QC-approximation

Figure 5: Energy repartition in time

Moreover, in Figure 6(a), important discontinuities appears on the u_x displacement fields due to the reflections. In the country, in Figure 6(b), the nonlocal domain has not be polluted by any spurious reflections.

3 Fine coarse scale decomposition

In this section we present how to obtain an equivalent coarse model based on a finite element approximation. Then, we propose a coupling method permeable for the macro informations and absorbing for the micro informations in order to avoid spurious reflections. Finally some results are presented on 1D problems.

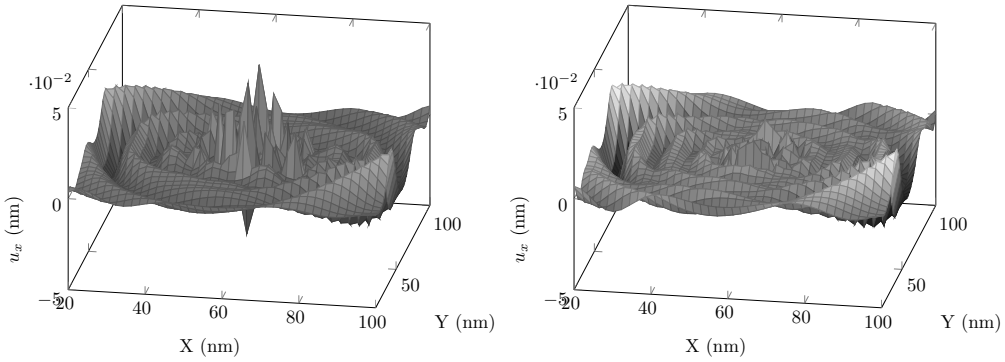

(a) Inconsistent QC-approximation (b) Consistent QC-approximation

Figure 6: u_x displacement at time step 150

3.1 Coarse model

As it is not possible to use the fine model in the whole simulation due to the computational cost, we want to introduce a coarse model that enable to represent the macro part of the displacement field (see Figure 7). The main issue is to enable exchanges of macro informations between the fine and the coarse model without generating spurious phenomena.

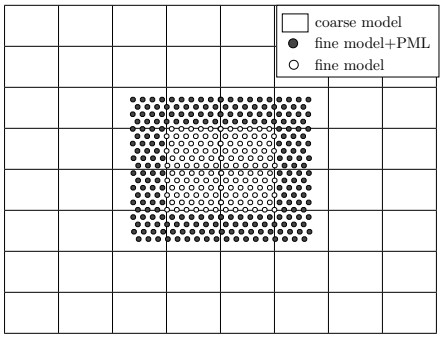

Figure 7: Fine and coarse models superposition

The Lagrangian description of the fine model is written as

$$\mathcal{L} = \frac{1}{2}\sum_{i=1}^{N} m_i \dot{u}_i^2 + \sum_{i=1}^{N}\sum_{j\neq i} E_{ij}(\mathbf{u}) - \sum_{i=1}^{N} f_i^{ext} u_i \quad \text{with} \quad u_i = x_i - X_i, \tag{13}$$

where m_i and f_i^{ext} are respectively the mass and external forces applied on the i^{th} particle. An equivalent formulation of (13) is :

$$\mathcal{L} = \frac{1}{2}\dot{\mathbf{u}}^T \mathbb{M}\dot{\mathbf{u}} + E^{tot}(\mathbf{u}) - (\mathbf{F}^{ext})^T \mathbf{u}, \tag{14}$$

where $\mathbb{M}$ is the mass matrix and $\mathbf{F}^{ext}$ is the external force vector.

In order to obtain the coarse model, we suppose that displacements can be written as a sum of micro and macro displacements [13] :

$$\mathbf{u} = \mathbf{u}_m + \mathbf{u}_M, \tag{15}$$

where $\mathbf{u}_m$ and $\mathbf{u}_M$, respectively represent the micro and macro displacements. We note $\mathbb{P}$ and $\mathbb{Q}$ the two projectors such that

$$\begin{cases} \mathbf{u}_M = \mathbb{P}\mathbf{u} \\ \mathbf{u}_m = \mathbb{Q}\mathbf{u} \end{cases} \quad \text{with} \quad \mathbb{P} + \mathbb{Q} = \mathbb{I}, \tag{16}$$

where $\mathbb{P}\mathbb{P} = \mathbb{P}$ and $\mathbb{P}\mathbb{Q} = \mathbb{O}$.

A finite element approximation is use to define the macro model, hence the macro displacement correspond to

$$\mathbf{u}_M = \mathbb{N}\mathbf{u}_{FE}, \tag{17}$$

where $\mathbf{u}_{FE}$ is the nodal displacement vector and $\mathbb{N}$ is the matrix of shape functions that interpolate the displacement of the initial particle positions.

Hence, combining (15) and (16) we can define the macro projector $\mathbb{P}$ such that

$$\mathbb{P}\mathbf{u} = \mathbb{N}\mathbf{u}_{FE}, \tag{18}$$

which yields

$$\mathbb{P} = \mathbb{N}\left(\mathbb{N}^T\mathbb{N}\right)^{-1}\mathbb{N}^T. \tag{19}$$

We obtain the Lagrangian description of the macro model using (17) and (13) :

$$\mathcal{L}_M = \frac{1}{2}\dot{\mathbf{u}}_M^T\mathbb{M}\dot{\mathbf{u}}_M + E^{tot}(\mathbf{u}_M) - (\mathbf{F}^{ext})^T\mathbf{u}_M \tag{20}$$

$$= \frac{1}{2}\dot{\mathbf{u}}_{FE}^T\mathbb{M}_{FE}\dot{\mathbf{u}}_{FE} + E^{tot}(\mathbb{N}\mathbf{u}_{FE}) - (\mathbf{F}_{FE}^{ext})^T\mathbf{u}_{FE} \tag{21}$$

where $\mathbb{M}_{FE} = \mathbb{N}^T\mathbb{M}\mathbb{N}$ is the macro mass matrix and $\mathbf{F}_{FE}^{ext} = \mathbb{N}^T\mathbf{F}^{ext}$ is the macro external force vector. Finally, the equation of motion of the macro model obtained from (21) is :

$$\mathbb{M}_{FE}\ddot{\mathbf{u}}_{FE} = -\frac{\partial E^{tot}(\mathbb{N}\mathbf{u}_{FE})}{\partial(\mathbb{N}\mathbf{u}_{FE})}\mathbb{N} + \mathbf{F}_{FE}^{ext} \tag{22}$$

3.2 Perfectly mathed Layer

As we only couple the macro scale of the displacement field, micro scale of the displacement from the fine model is not transmited to the coarse model and it can be reflected. In order to avoid such reflections, we add a perfectly match layer (PML) on the boundaries of the fine model (see Figure 7). Using (13), we obtain the following equation of motion :

$$m_i\ddot{u}_i = -\frac{\partial E^{tot}(\mathbf{u})}{\partial u_i} + f_i^{ext} \tag{23}$$

We suppose $f_i^{ext} = 0$ in the perfectly matched layer, the Fourier transformed of (23) is :

$$m_i \left(-i\omega\right)^2 u_i = -\frac{\partial E^{tot}(\mathbf{u})}{\partial u_i}. \tag{24}$$

The perfectly matched layer is constructed by converting the real coordinates into complex coordinates as a function of frequency ω [11, 12]. Hence, the following operation is performed :

$$\partial u_i \rightarrow \left(1 + \frac{d(x_p)}{-i\omega}\right)^2 \partial u_i, \tag{25}$$

where $d(x_p)$ is the damping term that controls the damping as a function of x_p, the distance away from the PML boundary (see Figure 8). Combining (24) and (25), we obtain :

$$m_i \left(1 + \frac{d(x_p)}{-i\omega}\right)^2 \left(-i\omega\right)^2 u_i = -\frac{\partial E^{tot}(\mathbf{u})}{\partial u_i}. \tag{26}$$

Finally, by performing inverse Fourier transform on (26), the perfectly matched layer equation of motion becomes :

$$m_i \ddot{u}_i = -\frac{\partial E^{tot}(\mathbf{u})}{\partial u_i} - 2m_i d(x_p)\dot{u}_i - m_i d(x_p)^2 u_i, \tag{27}$$

which leads to

$$\mathbb{M}\ddot{\mathbf{u}} = -\frac{\partial E^{tot}(\mathbf{u})}{\partial \mathbf{u}} - 2\mathbb{M}\mathbb{D}\dot{\mathbf{u}} - \mathbb{M}\mathbb{D}^2\mathbf{u}, \tag{28}$$

where is $\mathbb{D}$ a diagonal matrix of the damping term $d(x_p)$.

3.3 Implementation

The same discretisation in time Δt is used in both coarse and fine models and a verlet algortihm is chosen to update the velocities and displacements at each time step.

Moreover, in region with the fine model without PML, we update the macro displacement of the coarse model by extracting the macro displacement from $\mathbf{u}$. The PML added to the fine model will absorb all informations from the fine scale. Thus, at each time step we update the macro displacement in the PML region with the macro displacement $\mathbf{u}_{FE}$ from the coarse model.

Finally, we use as similar algorithm as [13] to run the simulation :

1. Update displacements $\mathbf{u}^{n+1}$ and $\mathbf{u}_{FE}^{n+1}$:

$$\begin{pmatrix} \mathbf{u} \\ \mathbf{u}_{FE} \end{pmatrix}^{n+1} = \begin{pmatrix} \mathbf{u} \\ \mathbf{u}_{FE} \end{pmatrix}^{n} + \Delta t \begin{pmatrix} \dot{\mathbf{u}} \\ \dot{\mathbf{u}}_{FE} \end{pmatrix}^{n} + \frac{\Delta t^2}{2} \begin{pmatrix} \ddot{\mathbf{u}} \\ \ddot{\mathbf{u}}_{FE} \end{pmatrix}^{n} \tag{29}$$

2. Update velocity $\dot{\mathbf{u}}^{n+1(*)}$:

$$\dot{\mathbf{u}}^{n+1(*)} = \dot{\mathbf{u}}^{n} + \frac{\Delta t}{2}\ddot{\mathbf{u}}^{n} \tag{30}$$

3. Compute accelerations $\ddot{\mathbf{u}}^{n+1}$ for $\ddot{\mathbf{u}}_{FE}^{n+1}$:

$$\ddot{\mathbf{u}}^{n+1} = \mathbb{M}^{-1}\left(\mathbf{F}_{ext} - \frac{\partial E^{tot}(\mathbf{u}^{n+1})}{\partial \mathbf{u}^{n+1}}\right) - \mathbb{D}^2\mathbf{u}^{n+1} - \mathbb{D}\dot{\mathbf{u}}^{n+1(*)} \tag{31}$$

$$\ddot{\mathbf{u}}_{FE}^{n+1} = \mathbb{M}_{FE}^{-1}\left(\mathbf{F}_{FE}^{ext} - \frac{\partial E^{tot}(\mathbb{N}\mathbf{u}_{FE}^{n+1})}{\partial \mathbb{N}\mathbf{u}_{FE}^{n+1}}\mathbb{N}\right) \tag{32}$$

4. Update velocities $\dot{\mathbf{u}}^{n+1}$ and $\dot{\mathbf{u}}_{FE}^{n+1}$:

$$\begin{pmatrix} \dot{\mathbf{u}} \\ \dot{\mathbf{u}}_{FE} \end{pmatrix}^{n+1} = \begin{pmatrix} \dot{\mathbf{u}} \\ \dot{\mathbf{u}}_{FE} \end{pmatrix}^{n} + \frac{\Delta t}{2}\left[\begin{pmatrix} \ddot{\mathbf{u}} \\ \ddot{\mathbf{u}}_{FE} \end{pmatrix}^{n} + \begin{pmatrix} \ddot{\mathbf{u}} \\ \ddot{\mathbf{u}}_{FE} \end{pmatrix}^{n+1}\right] \tag{33}$$

5. Cross macro scales :

$$\begin{cases} \mathbb{N}\mathbf{u}_{FE} = \mathbb{P}\mathbf{u} \\ \mathbb{N}\dot{\mathbf{u}}_{FE} = \mathbb{P}\dot{\mathbf{u}} \end{cases} \quad \text{in the fine model} \tag{34}$$

$$\begin{cases} \mathbf{u} = \mathbb{N}\mathbf{u}_{FE} + \mathbb{Q}\mathbf{u} \\ \dot{\mathbf{u}} = \mathbb{N}\dot{\mathbf{u}}_{FE} + \mathbb{Q}\dot{\mathbf{u}} \end{cases} \quad \text{in the PML} \tag{35}$$

3.4 Application

To evaluate the reductions of spurious reflections, we use this method on 1D problems as defined in Figure 8. We use 120 particles in the fine model (PML included). The size L of the coarse element is equal to $20 \times r_0$, 10 elements are used in the overlapping region that include the elements needed for the PML.

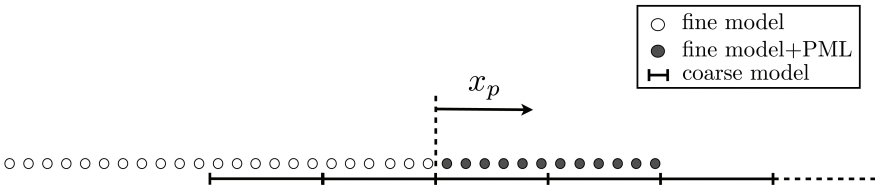

Figure 8: Definition of the 1D problem

We generate incident waves with different wavelengths in the fine model, then we calculate the parts of this initial energy that have been reflected, transmitted and absorbed by the fine-coarse scale interface. In Figures 9 and 10, we see some examples of incident wave before and after passing the fine-coarse scale interface.

As illustrated in Figure 11, we note that for short wavelength, almost all the initial energy have been absorbed, and globally we avoid any reflection at the fine-coarse scale interface. In the case of large wavelenghts, the initial energy is transmitted to the coarse model without dissipations. Nevertheless, for short-large wavelengths, the energy of the system is increased by the passing over the interface which has no physical meaning. Hence, this point should be the object of further works.

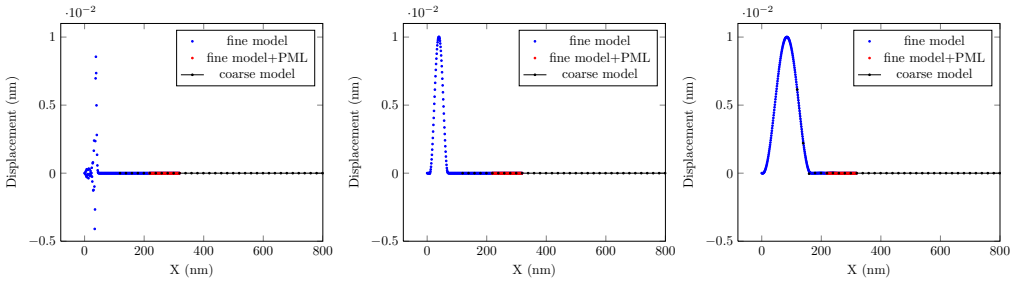

(a) (b) (c)

Figure 9: Initial incident waves

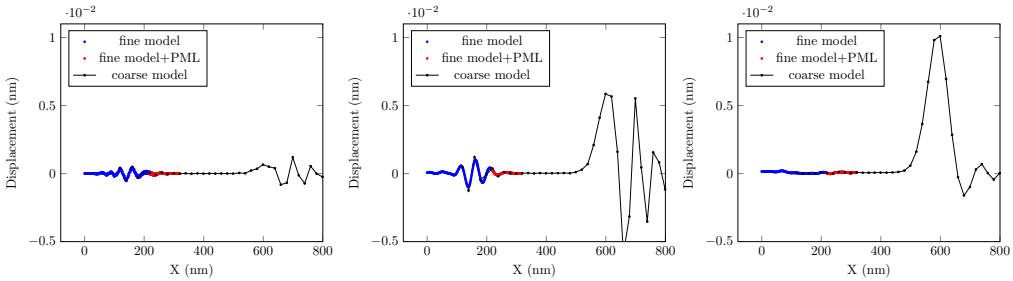

(a) (b) (c)

Figure 10: Incident waves after reaching the interface

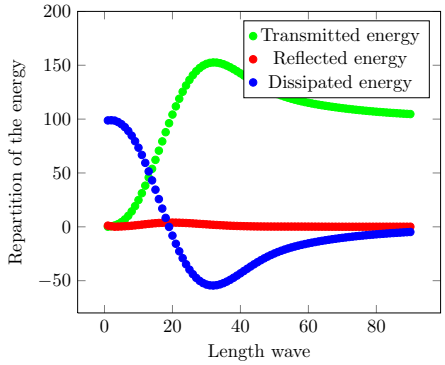

Figure 11: Repartition of the energy after the wave reached the interface

4 Conclusions

We explored and proposed solutions to the two different mechanisms responsible for spurious phenomena in dynamics. The proposed NL2L scheme based on a QC-approximation shows relevant results on 2D dynamics simulations to avoid reflections at local/nonlocal interfaces. In the case of fine/coarse interfaces, the first results point out that we are also able to avoid spurious reflections. Nevertheless further studies are needed to understand and to control the rise of energy for large wavelenghts.

References

[1] F.K. Wittel, F. Kun and H.J. Herrmann, Particle Models: Simulation of Damage and Fracture in Composites using a Discrete Element Approach, G. Busse, B. Kröplin, and FK Wittel: Damage and its Evolution in Fiber-Composite Materials: Simulation and Non-Destructive Evaluation, BoD, 2006.

[2] W.A. Curtin and R.E. Miller, Atomistic/continuum coupling in computational materials science, Modelling and simulation in materials science and engineering, 11:R33, 2003.

[3] E.B. Tadmor, M. Ortiz and R. Phillips, Quasicontinuum analysis of defects in solids, Philosophical Magazine, 73(6):1529–1564, 1996.

[4] V.B. Shenoy, R. Miller, E.B. Tadmor, D. Rodney, R. Phillips and M. Ortiz, An Adaptive Methodology for Atomic Scale Mechanics-The Quasicontinuum Method, Journal of the Mechanics and Physics of Solids, 73:611–642, 1999.

[5] H. Ben Dhia, Problèmes mécaniques multi-échelles: la méthode Arlequin, Comptes Rendus de l'Académie des Sciences-Series IIB-Mechanics-Physics-Astronomy, 329(12):899–904, 1998.

[6] S.P. Xiao and T. Belytschko, A bridging domain method for coupling continua with molecular dynamics, Computer methods in applied mechanics and engineering, 193(17-20):1645–1669, 2004.

[7] G.J. Wagner and W.K. Liu, Coupling of atomistic and continuum simulations using a bridging scale decomposition, Journal of Computational Physics, 190(1):249–274, 2003.

[8] T. Shimokawa, J.J. Mortensen, J. Schiøtz and K.W. Jacobsen, Matching conditions in the quasicontinuum method: Removal of the error introduced at the interface between the coarse-grained and fully atomistic region, Physical Review B, 69:1-10, 2004.

[9] W. E, J. Lu and J.Z. Yang, Uniform accuracy of the quasicontinuum method, Physical Review B, 74(21):1-12, 2006.

[10] J. Marchais, C. Rey and L. Chamoin, Geometrically consistent approximations of the energy for the reduction of nonlocal particle models in the quasicontinuum framework, submitted.

[11] J.P. Berenger, A perfectly matched layer for the absorption of electromagnetic waves, Journal of computational physics, 114(2):185-200, 1994.

[12] W.C. Chew and Q.H. Liu, Perfectly matched layers for elastodynamics: a new absorbing boundary condition, Urbana, 51:61801, 1996.

[13] A.C. To and S. Li, Perfectly matched multiscale simulations, Physical Review B, 72(3):035414, 2005.